

A method for evaluating the combustion efficiency in direct connect supersonic combustion test facilities

A. Reggiori, G. Riva, G.B. Daminelli

CNR-TEMPE, Via R. Cozzi 53, 20125 Milano, Italy

Abstract: A method for analyzing supersonic combustion tests which takes into account the 3-D character of the flow at the combustor exhaust is presented. By this method, the efficiency of hydrogen combustion in a Mach 3, high-enthalpy air flow was evaluated under a variety of operating conditions. The experimental tests were conducted using a direct connect supersonic combustion pulse facility fed with vitiated air at 2 MPa and 2400 K. The combustion efficiency was evaluated on the basis of detailed pressure and Mach number maps on the combustor exhaust area. The Reynolds Analogy was used to model the heat losses at the tunnel walls. A large number of combustion tests were analyzed to evaluate the effectiveness of different flame stabilizers, placed either on the tunnel walls or in the flow core. Increments of the overall equivalence ratio (varied within the range 0.2 - 1) were found to improve the combustion efficiency. Nearly all tests with equivalence ratio above 0.6 gave combustion efficiencies in the range 0.5 - 1.

Key words: Supersonic combustion, Scramjets, Air-breathing engines

1. Introduction

Experimental tests on supersonic combustion are often carried out to provide, as one of the typical results, the combustion efficiency, which is defined as the ratio between actual and maximum energy release in case of fuel or oxygen complete consumption. The chemical analysis of the combustion products is the most direct method to evaluate the combustion efficiency, however gas sampling may have problems of time resolution (especially in pulse facilities), quenching and condensation inside the probes, and cost of gas analyzers.

An alternative technique relies on static and total pressure measurements at different locations along the supersonic tunnel. These data allow the construction of static pressure and Mach number maps, whose analysis provide the combustion efficiency and all the thermodynamic variables of concern. In all cases, both experimental measurements and data analysis should take into account the intrinsic 3-D nature of the flow (Billig (1993)). In fact, at a given axial location, both

static and pitot pressures (as well as the gas chemical composition) may change significantly, depending on the probe position. These non uniform distributions of the flow thermophysical and chemical properties are mainly due to the presence of shock waves, wakes of structures placed into the channel (flame stabilizers and injector struts) and boundary layer.

This paper describes a method for analyzing supersonic combustion tests based on pressure measurements, which accounts for the 3-D nature of the flow at the combustor exhaust, and allows a reliable evaluation of the combustion efficiency. Hydrogen combustion tests in a Mach 3, high enthalpy air flow were carried out using the CNR-TEMPE supersonic combustion pulse facility (Riva et al. (1997-a) and Riva et al. (1997-b)) and analyzed using such a method.

2. Experimental setup and procedure

A general layout of the supersonic combustion pulse facility is given in Fig. 1. The supersonic tunnel is fed with high enthalpy vitiated air coming from a 15 liters volume, 4 m length free piston compression tube, in which the effects of rapid compression and hydrogen precombustion are combined to produce stagnation temperature of about 2000-2500 K, and pressure up to 7-8 MPa. These thermodynamic conditions are obtained inside a 1.3 liters volume stainless steel vessel (stagnation vessel), in which the air is forced through a check valve. The high enthalpy vitiated air (20% volume of water content) is then sent to the isentropic nozzle through a calibrated hole, 7 mm diameter, in order to reduce the stagnation pressure and prolong the blowdown transient. Downstream of the nozzle, the tunnel has constant rectangular cross sectional area, 26x30 mm. This part of the tunnel is 300 mm long, and acts as an isolator, to prevent the nozzle unstart due to thermal choking. A divergent follows, 600 mm length, 30 mm width, 6 deg. angle (Fig. 2). The divergent exhaust is connected to a large vessel, 200 liters volume, in which vacuum conditions are permanently set. Hydrogen is injected immediately before the beginning of the divergent, normally to the air flow, through two series of 5 equally spaced holes, 0.8 mm diameter, from the top and bottom walls.

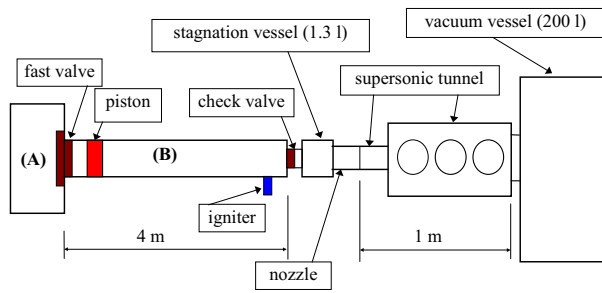


Figure 1. Scheme of the CNR-TEMPE supersonic combustion pulse facility.

A number of calibration tests were performed to correlate the initial composition of the $air - H_2 - O_2$ mixture fed in the free piston compressor to the thermodynamic conditions obtained in the stagnation vessel. Such tests demonstrated that air at 4 MPa in the compressor reservoir (A), and an initial charge consisting of 0.12 MPa of air and 0.048 MPa of $H_2 - O_2$ stoichiometric mixture in the pump tube (B) (Fig. 1), systematically produced 8 MPa and 2400 K in the stagnation vessel. In all combustion tests, static pres-

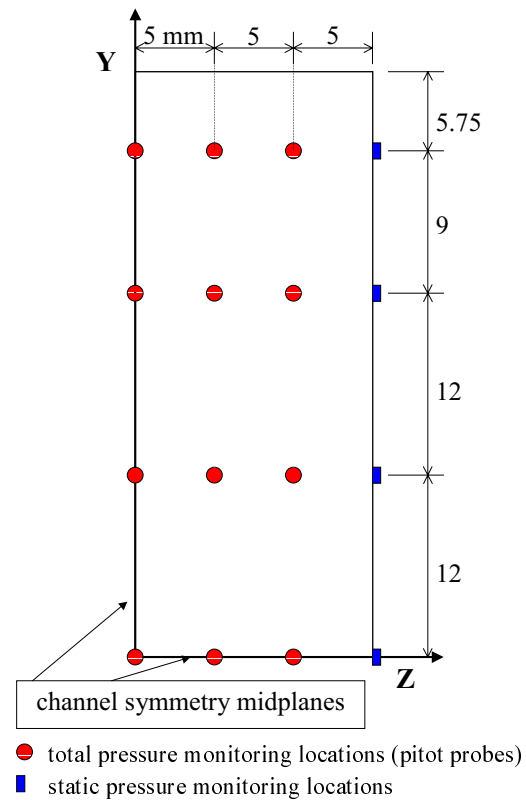


Figure 3. Pitot and static pressure probes position at the tunnel exhaust.

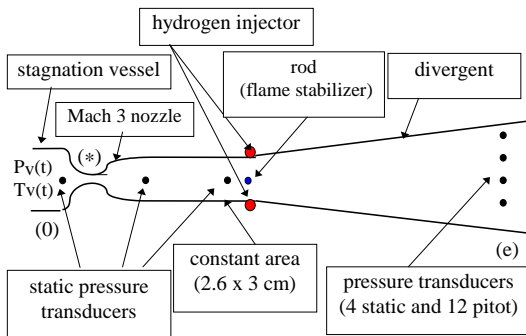


Figure 2. Qualitative sketch of the supersonic tunnel.

sure is monitored at several axial locations along the tunnel: stagnation vessel, nozzle exit, tunnel exhaust (Fig. 2). Twelve pitot probes are mounted near the tunnel exhaust (500 mm downstream of the hydrogen injectors), where four probes detect the static pressure at different distances from the channel horizontal mid-plane. This probes distribution takes advantage of the symmetry with respect to the channel midplanes, and provides a rather detailed map of the Mach number over the tunnel exhaust cross sectional area (Fig. 3).

Hydrogen is injected during the early period of the stagnation vessel discharge, when pressure and temperature levels allow autoignition. The injection usually lasts 30-50 ms, the total blowdown time being of the order of 200-300 ms. Pressure data acquisition is performed by multi-channel digital transient recorders, 12 bit resolution, 1 or 10 MHz maximum sampling frequency per channel. Static pressure measurements along the isolator and at the tunnel exhaust employ transducers with 0.7 MPa full scale, 1 MHz natural frequency, $\pm 1\%$ global accuracy. The pressure inside the stagnation vessel is measured using a 10 MPa full scale transducer, 150 kHz natural frequency, $\pm 0.3\%$ global accuracy.

3. Combustion tests analysis

For each test, the following experimental data set is available:

- pressure in the stagnation vessel, p_v , (measured, time dependent);
- maximum temperature in the stagnation vessel, $T_{v,max}$ (2400 K, known from calibration);

- static pressure at nozzle exit, p_f , (measured, time dependent);
- static pressure (4 monitoring points) at the tunnel exhaust (measured, time dependent);
- pitot/static pressure ratio at 12 locations on the channel exhaust cross sectional area (measured, time dependent);
- hydrogen injection stagnation pressure, p_{H_2} , (measured, time dependent);
- hydrogen injection stagnation temperature, T_{H_2} , (from calibration and measurements, time dependent);
- tunnel geometry.

Pressure and temperature decay inside the stagnation vessel has a characteristic time of the order of 100 ms, while the air residence time in the supersonic tunnel is about 1 ms or less. This means that, during the residence time, the upstream conditions do not significantly change, and thus the discharge transient can be described with a sequence of time steps, each considered as a quasi-steady state.

3.1. Calculation of the stagnation vessel time dependent temperature

The calibration tests show that the maximum temperature achieved in the stagnation vessel is 2400 K, with a corresponding maximum pressure of about 8 MPa. Such conditions are fundamental for scaling the transient thermal and fluid dynamic field in the tunnel. The time history of the stagnation vessel temperature is obtained from continuity and state equations:

$$T_v(t) = \frac{p_v(t)}{p_{v,max}} \frac{T_{v,max}}{\left(1 - \frac{\sqrt{R_v T_{v,max}}}{2} \int_{t_i}^t H_v \sqrt{\frac{p_v(t)}{p_{v,max}}} dt\right)^2} \quad (1)$$

where t_i is the time at which the pressure features its maximum and

$$H_v = \frac{A_v}{V_v} \left[\gamma_v \left(\frac{2}{\gamma_v + 1} \right)^{\frac{\gamma_v + 1}{\gamma_v - 1}} \right]^{1/2} \quad (2)$$

3.2. Flow characterization in the Mach 3 nozzle

The air temperature variations lead to a change in time and space of the air thermophysical properties (e.g., the specific heats ratio, γ), and to a change in time of the Mach number at the nozzle exit, being the nozzle geometry based on a constant value of γ (i.e., $\gamma = 1.3$). A further problem is the evaluation of the total temperature decrement which may occur along the path between stagnation vessel and nozzle throat: in fact, the high temperature air impacts cold surfaces

and lowers its temperature before reaching the nozzle. The air mass flow per unit area is computed assuming choked flow through the 7 mm diameter exhaust of the stagnation vessel:

$$\dot{m}_{a,v} = \frac{p_v}{\sqrt{T_v}} \sqrt{\frac{\gamma_v}{R_v}} \left(\frac{2}{\gamma_v + 1} \right)^{\frac{\gamma_v + 1}{2(\gamma_v - 1)}} \quad (3)$$

The flow along the nozzle divergent is assumed adiabatic. The known quantities are: stagnation vessel pressure, p_v ; stagnation vessel temperature, T_v ; chemical composition of the vitiated air; static pressure at the isentropic nozzle exhaust, p_f ; nozzle geometry.

The quantities to be determined are: throat static pressure, p_* ; throat total temperature, $T_{t,*}$; Mach number at the nozzle exhaust, M_f ; average specific heats ratio in the nozzle divergent, $\bar{\gamma}$.

The solution is obtained according to the following procedure:

- A starting value of $\bar{\gamma}$ is assumed
- M_f is computed by iteration procedure from:

$$\frac{A_f}{A_*} = \frac{1}{M_f} \left(\frac{1 + \frac{\bar{\gamma} - 1}{2} M_f^2}{\bar{\gamma} + 1} \right)^{\frac{\gamma_v + 1}{2(\gamma_v - 1)}} \quad (4)$$

- p_* is computed from Eq. 4 and mass conservation, under adiabatic conditions:

$$p_* = p_f \left(\frac{2 + (\bar{\gamma} - 1) M_f^2}{\bar{\gamma} + 1} \right)^{\frac{\bar{\gamma}}{\bar{\gamma} - 1}} \quad (5)$$

- Mass conservation is used to calculate the throat static temperature:

$$T_* = \frac{\gamma_*}{R_v} \left(\frac{p_* A_*}{A_v \dot{m}_{a,v}} \right)^2 \quad (6)$$

where $\gamma_* = \bar{\gamma}$ is assumed as a first guess.

- $\gamma_* = \gamma(T_*, \text{chemical composition})$ is computed.
- The end divergent static temperature is computed using the assumption of adiabatic flow:

$$T_f = T_* \frac{\gamma_* + 1}{2 + (\gamma_f - 1) M_f^2} \quad (7)$$

where $\gamma_f = \bar{\gamma}$ is assumed as a first guess.

- $\gamma_f = \gamma(T_f, \text{chemical composition})$ is computed.
- $\bar{\gamma}_{new} = (\gamma_* + \gamma_f)/2$ is computed.
- Convergence test: $|\bar{\gamma} - \bar{\gamma}_{new}| < 10^{-3}$
- If the convergence test above is not met, $\bar{\gamma}_{new}$ is used as a restarting value, and the procedure is repeated from the second step.
- When convergence is achieved, the total temperature $T_{t,f} \equiv T_{t,*}$ is computed, since M_f is known.

3.3. Gas flow chemical composition

An algebraic expression can be devised to correlate gas composition (in terms of components partial pressures), combustion efficiency, and equivalence ratio:

$$p_t = p_{N_2,i} + p_{H_2O,i} + E\eta_c p_{H_2,st} + (1 - E\eta_c)p_{O_2,i} + E(1 - \eta_c)p_{H_2,st} \quad (8)$$

where the equivalence ratio is

$$E = \frac{(A/F)_{st}}{(A/F)} \quad (9)$$

In the equations above, the subscripts "i" and "st" refer to "initial" and "stoichiometric" conditions. The partial pressures of the main gas components are:

- $p_{N_2} = p_{N_2,i}$;
- $p_{H_2O} = p_{H_2O,i} + E\eta_c p_{H_2,st}$;
- $p_{O_2} = (1 - E\eta_c)p_{O_2,i}$;
- $p_{H_2} = E(1 - \eta_c)p_{H_2,st}$;

The correlations above are used to evaluate the gas mixture average thermophysical properties (e.g., specific heats, gas constant). Fitting functions are used for the temperature dependent specific heats of each component.

3.4. Mass and energy balances

Assuming as control surfaces the nozzle throat cross sectional area (subscript "n") and the tunnel exhaust cross sectional area (subscript "e"), the following energy balance holds:

$$(\bar{c}_{p,a}T_{t,a}\dot{m}_aA)_* + (c_pT_t\dot{m}A)_{H_2} + \dot{Q}_c - \dot{Q}_w = \int_{A_e} \bar{c}_{p,e}T_{t,e}\dot{m}_e dA \quad (10)$$

The left hand side of Eq. 10 includes four terms, which model, respectively, the vitiated air total enthalpy flow crossing the nozzle throat, the fuel total enthalpy flow, the heat released by combustion, and the heat losses at the tunnel walls. The right hand side term is the total enthalpy flow at the tunnel exhaust. At the nozzle throat, the vitiated air total enthalpy flow can be computed as:

$$(\bar{c}_{p,a}T_{t,a}\dot{m}_aA)_* = \frac{p_*A_*}{\gamma_* - 1} \gamma_*^{\frac{3}{2}} \frac{\gamma_* + 1}{2} \sqrt{R_*T_*} \quad (11)$$

The fuel total enthalpy flow is modeled assuming choked flow across the injector openings:

$$(c_pT_t\dot{m}A)_{H_2} = (c_pT_tA)_{H_2} \frac{p_{t,H_2}}{\sqrt{T_{t,H_2}}} \sqrt{\frac{\gamma_{H_2}}{R_{H_2}}} \left(\frac{2}{\gamma_{H_2} + 1}\right)^{\frac{\gamma_{H_2} + 1}{2(\gamma_{H_2} - 1)}} \quad (12)$$

where the adiabatic expansion law is used to correlate total temperature and pressure. According with the definition of combustion efficiency, we can write the energy release rate of the combustion process as:

$$\dot{Q}_c = \eta_c \dot{Q}_{c,max} \quad (13)$$

The maximum energy release rate, $\dot{Q}_{c,max}$, has two different formulations, depending on the range of the equivalence ratio. For lean mixtures ($E \leq 1$), $\dot{Q}_{c,max} = (\Delta H_f \dot{m}A)_{H_2}$, and for rich mixtures ($E \geq 1$), $\dot{Q}_{c,max} = (\Delta H_{f,H_2} \dot{m}_{a,*}) / (A/F)_{st} A_*$. The heat lost at the tunnel wall (assumed isothermal, $T_w = 300K$) is:

$$\dot{Q}_w = \dot{m}_{a,*} A_* \bar{c}_{p,a} \Delta T_{t,const} + (\dot{m}_{a,*} A_* + \dot{m}_{H_2} A_{H_2}) \bar{c}_{p,div} \Delta T_{t,div} \quad (14)$$

The Reynolds analogy (Schlichting (1960)) provides an estimate of the total temperature decay due to the thermal boundary layer, based on the friction coefficient, c_f . The total temperature decay in the constant area channel is:

$$\Delta T_{t,const} = (T_{t,*} - T_w) \left(1 - e^{-\frac{c_f(a+b)(x_0 - x_*)}{a b Pr}}\right) \quad (15)$$

The total temperature decay in the divergent is:

$$\Delta T_{t,div} = (T_{t,0} - T_w) \left(1 - e^{-\frac{c_f}{Pr} \left(\frac{x_e - x_0}{a} + \frac{1}{k} \ln \frac{b_e}{b_0}\right)}\right) \quad (16)$$

In the equations above, a is the (constant) channel width, b is the channel height, Pr is the Prandtl number, and $k = db/dx$. The total enthalpy flow at the tunnel exhaust, where the thermal and fluid dynamic boundary layers may be rather thick, is evaluated using the detailed pressure and Mach number maps detected with static and pitot pressure probes.

$$\int_{A_e} \bar{c}_{p,e} T_{t,e} \dot{m}_e dA = \int_{A_e} \frac{p_e M_e}{\bar{\gamma}_e - 1} \bar{\gamma}_e^{\frac{3}{2}} \left(1 + \frac{\bar{\gamma}_e - 1}{2} M_e^2\right) \sqrt{R_e T_e} dA \quad (17)$$

All terms included in Eq. 10 have now been defined. Combining Eq. 10 and Eq. 13, the following expression of the combustion efficiency is obtained:

$$\eta_c = \frac{1}{\dot{Q}_{c,max}} \left[\int_{A_e} \bar{c}_{p,e} T_{t,e} \dot{m}_e dA + (\bar{c}_{p,a}T_{t,a}\dot{m}_aA)_* - (c_pT_t\dot{m}A)_{H_2} + \dot{Q}_w \right] \quad (18)$$

Both vitiated air and hydrogen mass flows are evaluated from experiments. Mass conservation relates such experimental values with the total mass flow at the tunnel exhaust:

$$(\dot{m}_aA)_* + (\dot{m}A)_{H_2} = \int_{A_e} \frac{p_e M_e}{\sqrt{T_{t,e}}} \sqrt{\frac{\bar{\gamma}_e}{R_e}} \left(1 + \frac{\bar{\gamma}_e - 1}{2} M_e^2\right) dA \quad (19)$$

An accurate solution of Eqns. 18 and 19 must consider the total temperature and Mach number distributions on the exhaust cross sectional area, boundary layer included. To do this, some assumptions have to be made, and, in particular, changes of the ratio p_t/p are assumed linear between two adjacent pitot probes, and parabolic between the wall (where $p_t/p = 1$, that is $M = 0$) and the nearest pitot probe. The total temperature is assumed constant in the flow core (i.e., the portion of the exhaust area covered by the array of pitot probes). Near the wall, the following correlation between total temperature and gas velocity is adopted:

$$T_{t,e} = T_w + (T_{t,e,core} - T_w) \frac{u_e}{u_{e,core}} \quad (20)$$

Eq. 20 is based on the Reynolds analogy, and is rigorous for $Pr = 1$, $dp/dx = 0$, and constant wall temperature. Algebraic manipulation leads to the following implicit form:

$$T_{t,e} = T_w + (T_{t,e,core} - T_w) \frac{M_e}{M_{e,core}} \sqrt{\frac{\frac{T_{t,e}}{T_{t,e,core}} \frac{\bar{\gamma}_e}{\bar{\gamma}_{e,core}} \frac{1 + \frac{\bar{\gamma}_{e,core}-1}{2} M_{e,core}^2}{1 + \frac{\bar{\gamma}_e-1}{2} M_e^2}}{1 + \frac{\bar{\gamma}_e-1}{2} M_e^2}} \quad (21)$$

3.5. Solution procedure

The purpose of the combustion tests analysis is the evaluation of the combustion efficiency as a function of time. Each test is considered as a sequence of quasi-steady states lasting 100 ms. Experimental data processed by a smoothing algorithm are provided every 100 μs , producing 1000 consecutive pressure fields. The pressure database includes static pressures at various monitoring locations (i.e., stagnation vessel, nozzle exit, tunnel exhaust, fuel injector). The total and static pressures at the tunnel exhaust are monitored in detail in order to build a map as accurate and complete as possible. At each time step, the following procedure is carried out.

- Upstream air stagnation temperature, T_v , is computed (sec. 3.1).
- Hydrogen total temperature, T_{t,H_2} , is computed (sec. 3.4).
- Nozzle Mach number and flow thermophysical properties are computed (sec. 3.3).
- Equivalence ratio, E , is computed (sec. 3.3)
- A first guess of the gas composition at the tunnel exhaust is made (e.g., no combustion, $\eta_c = 0$).
- A first guess of the total temperature in the flow core at the tunnel exhaust, $T_{t,e,core}$ is made.

- Mass conservation equation (Eq. 19) is solved.
- Test on the mass balance: errors above 0.1% lead to a further iteration, with a modified $T_{t,e,core}$.
- After mass balance convergence, the combustion efficiency, η_c , is computed (Eq. 18).
- Test on the difference between old and new values of η_c : a difference larger than 1% leads to the calculation of a new exhaust gas composition, based on the updated value of η_c (sec. 3.3), and to a new iteration restarting from the 6th step.
- After convergence, all relevant quantities (temperatures, gas composition, Mach numbers, combustion efficiency) are stored, and the analysis of the next time step is started.

4. Results

A preliminary parametric analysis, based on simplified equations, gave the influence on the combustion efficiency of inaccuracies in pressure data or test analysis: a 5% error on the combustor exhaust Mach number may lead to a 40% change of the combustion efficiency. Similar effects (30% change) are produced by a 5% variation of the exhaust static pressure. Particular attention was thus paid to experimental procedures and data analysis, in such a way as to minimize all inaccuracies.

A series of about 80 experimental tests was analyzed using a Fortran 77 computer code, specifically developed for this purpose, in which the solution procedure described in sec. 3.5 was implemented. In all tests, a Mach 3 nozzle was used to feed the supersonic tunnel. The tunnel geometry (divergent) was modified several times by inserting rods and steps of different size, at different axial locations, in order to enhance mixing and combustion stability. A few tests were carried out without hydrogen injection to estimate the average friction coefficient, c_f , responsible of the heat lost at the tunnel wall: $c_f = 0.007$ was selected and maintained for all combustion tests. The equivalence ratio was varied in the range 0.2 - 1, however, when stoichiometry was approached, flow choking and nozzle unstart occurred. As an example, results concerning a combustion test at relatively high equivalence ratio ($E = 0.76$) are given in Fig. 4 and Fig. 5. The first plot shows the time history of the total temperature in the stagnation vessel, at the nozzle throat, and at the tunnel exhaust (flow core). The temperature at the tunnel exhaust features a step, lasting about 30 ms, produced by the combustion process. The increment occurring at about 110 ms indicates the beginning of the tunnel unstart. The second plot provides the time evolution of gas specific heats ratio, γ , in the stagnation vessel

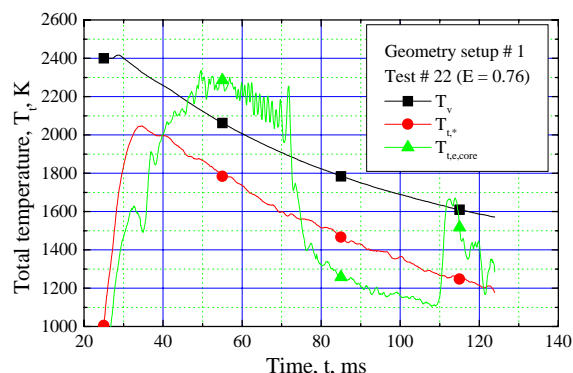


Figure 4. Upstream, nozzle, and exhaust total temperature evolution.

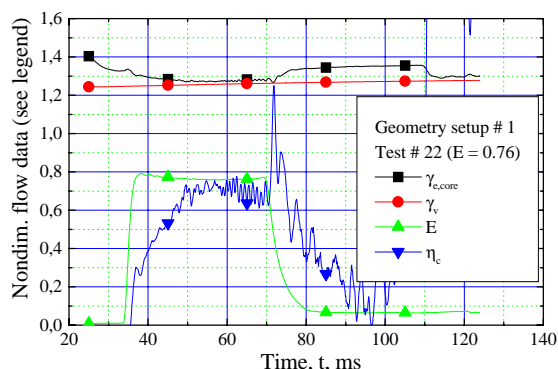


Figure 5. Time evolution of upstream and exhaust gas specific heats ratio, equivalence ratio, and combustion efficiency.

and at the tunnel exhaust, equivalence ratio, E , and combustion efficiency, η_c . In this case $\eta_c \cong 0.7$ was obtained in the flat region between 50 and 70 ms. The series of tests shows that high equivalence ratio often produced high combustion efficiency, while changes in the geometry setup did not produce relevant effects. This behaviour, shown in Fig. 6, where the test above is marked with a red solid spot, can be explained with the stronger perturbation of the supersonic flow introduced by increasing the hydrogen mass flow. Actually, near the hydrogen injector, shocks of strength proportional to the fuel mass flow are produced, leading to a local increment of pressure and temperature. Simultaneously, the gas speed decreases, and the residence time increases. All these effects contribute to enhance fuel-air mixing and to make ignition and combustion faster. Moreover, almost all tests were performed with high temperature hydrogen (up to 1000 K), and thus the local cooling effect was reduced.

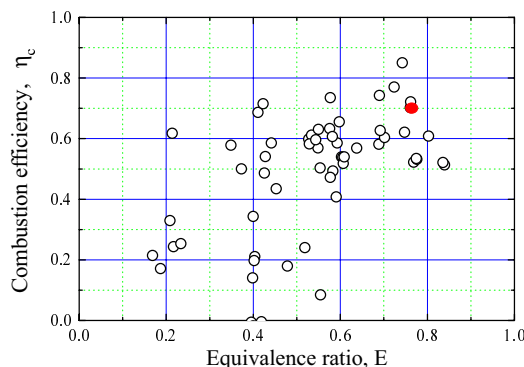


Figure 6. Effect of the equivalence ratio on the combustion efficiency.

5. Conclusions

A method for evaluating the combustion efficiency in direct connect supersonic combustion pulse facilities was developed and used to analyze a series of combustion tests in a Mach 3 high enthalpy air flow. The method accounts for the 3-D nature of the flow at the combustor exhaust and does not contain "tunable" parameters, leaving aside the gas friction coefficient, whose value can be set with calibration tests without fuel injection. The method is based on static and total pressure data, and provides the combustion efficiency and all relevant gas flow thermophysical properties. A series of tests was analyzed, to evaluate the effectiveness of different flame stabilizers, with equivalence ratio in the range 0.2 - 1. The results show that different flame stabilizers placed in the divergent, did not produce relevant changes in the combustion efficiency. The equivalence ratio, E , was found to be the most influencing parameter, as nearly all tests with $E > 0.6$ featured combustion efficiencies in the range 0.5 - 1.

Acknowledgement. This work was supported by the Italian Space Agency (ASI), Contract ARS-96-13.

References

- Billig FS (1993) Research on supersonic combustion. *Journal of Propulsion and Power*, 9, 4, 499–514
- Riva G, Reggiori A, Daminelli GB (1997-a) Hydrogen autoignition and combustion in supersonic flow at low equivalence ratio. *Journal of Propulsion and Power*, 13, 4, 532–537
- Riva G, Reggiori A, Daminelli GB (1997-b) High temperature hydrogen supply technique for supersonic combustion pulse facility. ISABE-97-7050. *Proceedings of the 13th ISABE*, 357–365
- Schlichting H (1960) *Boundary layer theory*, McGraw-Hill, New York.